Effect of quantum partial charges on the structure and dynamics of water in single-walled carbon nanotubes

Chang Y. Won, Sony Joseph, and N. R. Aluru[a)]
Department of Mechanical Science and Engineering, Beckman Institute for Advanced Science and Technology, University of Illinois at Urbana-Champaign, Urbana, Illinois 61801

(Received 20 March 2006; accepted 26 July 2006; published online 18 September 2006)

In this work, using quantum partial charges, computed from 6–31G**/B3LYP density functional theory, in molecular dynamics simulations, we found that water inside (6,6) and (10,0) single-walled carbon nanotubes with similar diameters but with different chiralities has remarkably different structural and dynamical properties. Density functional calculations indicate that tubes with different chiralities have significantly different partial charges at the ends of tubes. The partial charges at the ends of a (10,0) tube are around 4.5 times higher than those of a (6,6) tube. Molecular dynamics simulations with the partial charges show different water dipole orientations. In the (10,0) tube, dipole vectors of water molecules at the end of the tube point towards the water reservoir resulting in the formation of an *L* defect in the center region. This is not observed in the (6,6) tube where dipole vectors of all the water molecules inside the tube point towards either the top or the bottom water reservoir. The water diffusion coefficient is found to increase in the presence of the partial charges. Water in the partially charged (10,0) tube has a lower diffusion coefficient compared to that of in the partially charged (6,6) tube. © *2006 American Institute of Physics*.
[DOI: 10.1063/1.2338305]

I. INTRODUCTION

Ever since their discovery, carbon nanotubes (CNTs) have been an area of intense research, due to their unique chemical, electronic, and mechanical properties. CNTs can be filled with various materials making them one of the most promising candidates for many applications, such as sensors,[1,2] fuel storage,[3–5] and biological systems.[6] Since the size of a CNT is comparable to the size of a biological ion channel,[7] studies on water/electrolyte and CNT interaction have gained more attention because of their potential applications in biological nanosystems. Similarities in the structure of the hydrophobic channels of transmembrane proteins with CNTs suggest that the transport behavior of small molecules and ions through CNTs may parallel the transport through cell membrane proteins such as aquaporins.[8]

Molecular dynamics (MD) simulations by Hummer *et al.*[9] showed that water enters single-walled carbon nanotubes (SWCNTs) with a diameter as small as 8.1 Å at 300 K. Subsequently, several experimental studies have confirmed the wetting behavior of water inside nanotubes.[10,11] Rossi *et al.*[12] observed that confinement and interaction with the tube wall resulted in slow water dynamics. In order to understand the effect of confinement on the static and dynamic properties of water, several atomic scale simulations have been performed. MD simulations showed that water conducts through subnanometer (6,6) SWCNTs with the formation of a preferentially aligned water wire with each water dipole oriented in the same direction parallel to the nanotube axis.[9,13,14] In most classical MD simulations, carbon atoms in CNTs are modeled as neutral atoms with pairwise additive Lennard-Jones (LJ) potentials where the nanotube electronic properties are not considered. The effect of polarization of the nanotube on water transport properties is ignored in such an approach. Moulin *et al.*[15] calculated the polarization of CNTs of finite size immersed in liquid water by using a Lippmann-Schwinger-type equation. Density functional theory (DFT) and a self-consistent tight-binding method have been used for the calculation of the electronic properties and dielectric behavior of finite-length SWCNTs.[16] *Ab initio* MD simulations can capture the water-nanotube interactions more accurately.[17,18] However, a large computational cost prevents them from being used for studying water behavior under confinement beyond a few picoseconds of simulation time.

DFT calculations[19] on open-ended finite-length SWCNTs suggest that, at the nonsaturated end, C–C triple bonds are formed for armchair nanotubes causing a finite charge and a significant dipole moment at the tube ends. In zigzag carbon nanotubes, the C–C triple bonding is not observed at the ends.[20] This suggests that the chirality of the SWCNT could affect the nanotube electrostatics. Since water is a polar liquid, the tube chirality could influence the static and dynamic properties of confined water. To the authors' knowledge, the effect of chirality induced partial charges on the water structure and dynamics in finite length SWCNTs has not been reported previously in the literature.

In this work, to investigate the effect of chirality on water transport we considered two finite length (6,6) and (10,0) SWCNTs. They have similar confinement effects but different chiralities. Density functional calculations of the SWCNTs alone and the SWCNTs with water were performed to obtain quantum partial charges. The partial charges were

[a)]Author to whom correspondence should be addressed. Electronic mail: aluru@uiuc.edu. URL: https://netfiles.uiuc.edu/aluru/www/

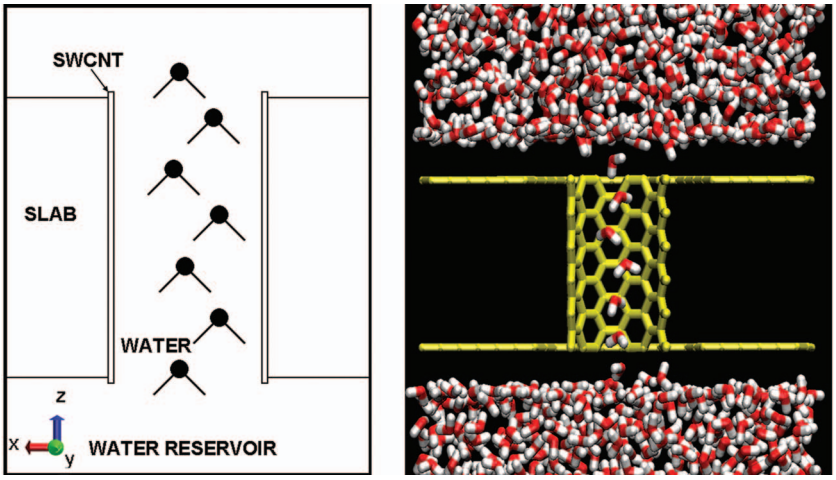

FIG. 1. (Color) Schematic (left) and visualization (right) of a single-walled carbon nanotube in a water bath.

then used in MD simulations to scrutinize water structure and transport, which are analyzed by computing the energy barriers. The rest of the paper is outlined as follows. First, we describe the DFT calculations and the MD simulations. The quantum partial charge results and the quantum and chirality effects on water structure and transport properties using the MD simulations are discussed next. Then the potential of mean force (PMF) analysis is presented, followed by the conclusions.

II. METHODS

The partial charge calculations were carried out by using the DFT method with the B3LYP model and the $6-31G^{**}$ basis. GAUSSIAN 03 (Ref. 21) was used to optimize the geometries and to calculate the partial charges. We considered two open-ended finite length SWCNTs—a (6,6) armchair SWCNT and a (10,0) zigzag SWCNT where water forms a single file. The (6,6) armchair SWCNT consisted of 132 carbon atoms with a length of 1.23 nm and a diameter of 0.8136 nm. The (10,0) zigzag SWCNT consisted of 120 carbon atoms and its length and diameter are 1.14 and 0.7829 nm, respectively. The initial C–C bond length was fixed at $d_{C-C}=1.42$ Å. To investigate the effect of water on the partial charges, we performed DFT calculations with and without water molecules inside the tubes. First, we obtained a geometry optimized structure by the AM1 semiempirical method. Han and Jaffe[22] found good agreement between carbon nanoconic tip energies and geometries from using the AM1 and DFT/B3LYP method. Recent results have shown that with $B3LYP/3-21G^{*}$, the CNT geometry matches well with experiments[23] and $B3LYP/6-31G^{*}$ model gives a good agreement with the experimental geometry of a fullerene derivative.[24] We performed the partial charge calculations with $B3LYP/6-31G^{**}$ using the geometry optimized structures. The partial charges on the SWCNT were obtained by fitting the electrostatic potential to fixed charge at the carbon atoms using the CHELPG scheme.[25] The CHELPG charges are suited for MD simulations because they capture higher order effects arising from dipoles and multipoles, though in an approximate way.

MD simulations were performed using modified GROMACS 3.2.1.[26] The system consisted of the SWCNT, water, and a slab. The SWCNT was fixed in the slab as shown in Fig. 1. The slab consisted of pseudoatoms mimicking the interior of a hydrophobic phospholipid bilayer.[27] This system was replicated periodically in all the three dimensions. The simulation box was $3.36\times3.234\times5.82$ nm^3. The reservoirs were initially filled with water. The extended simple point charge (SPC/E) model[28] with an oxygen atom of $-0.8476e$ charge and the two hydrogen atoms of $+0.4238e$ charge was used in the simulations. The OH bond length of 1.0 Å and the HOH bond angle of 109.47° were constrained by the SETTLE algorithm.[29] SPC/E model has been used successfully in simulating water in complex biomolecular environments such as gramicidin channels with single water wires.[30] The simulation box contained approximately 1500 water molecules. The Berendsen thermostat[31] with a time constant of 0.5 ps was employed to regulate the temperature at 300 K. The Berendsen pressure coupling with a time constant of 5.0 ps and a compressibility of 4.5×10^{-5} bar^{-1} maintained the system at 1 bar. The Lennard-Jones parameters for the interaction between carbon atoms were taken from Ref. 32 ($\sigma_{C-C}=0.3390$ nm, $\epsilon_{C-C}=0.2897$ kJ/mol), interactions between oxygen atoms were taken from the GROMACS force field[26] ($\sigma_{O-O}=0.3169$ nm, $\epsilon_{O-O}=0.6502$ kJ/mol), and parameters for atoms in the slab were taken from Ref. 13 ($\sigma_{slab-slab}=0.3871$ nm, $\epsilon_{slab-slab}=0.4909$ kJ/mol). Neutral carbon atoms and carbon atoms with the partial charges were employed in separate simulations to investigate the effect of partial charges. Particle mesh Ewald (PME) method with a 10 Å real-space cutoff, 1.5 Å reciprocal space gridding, and splines of order 4 with a 10^{-5} tolerance was implemented to compute electrostatic interactions. The equations of motion were integrated by using a leapfrog algorithm and the simulation time step was 2.0 fs. After an equilibration time of 1 ns, the simulations were continued for another 28 ns to obtain enough statistical sampling to calculate the transport properties.

III. RESULTS AND DISCUSSION

A. Partial charges

Figure 2 shows the CHELPG partial charges for the (6,6) armchair and the (10,0) zigzag SWCNTs along the axis of the tube. The charges were averaged for atoms with the same

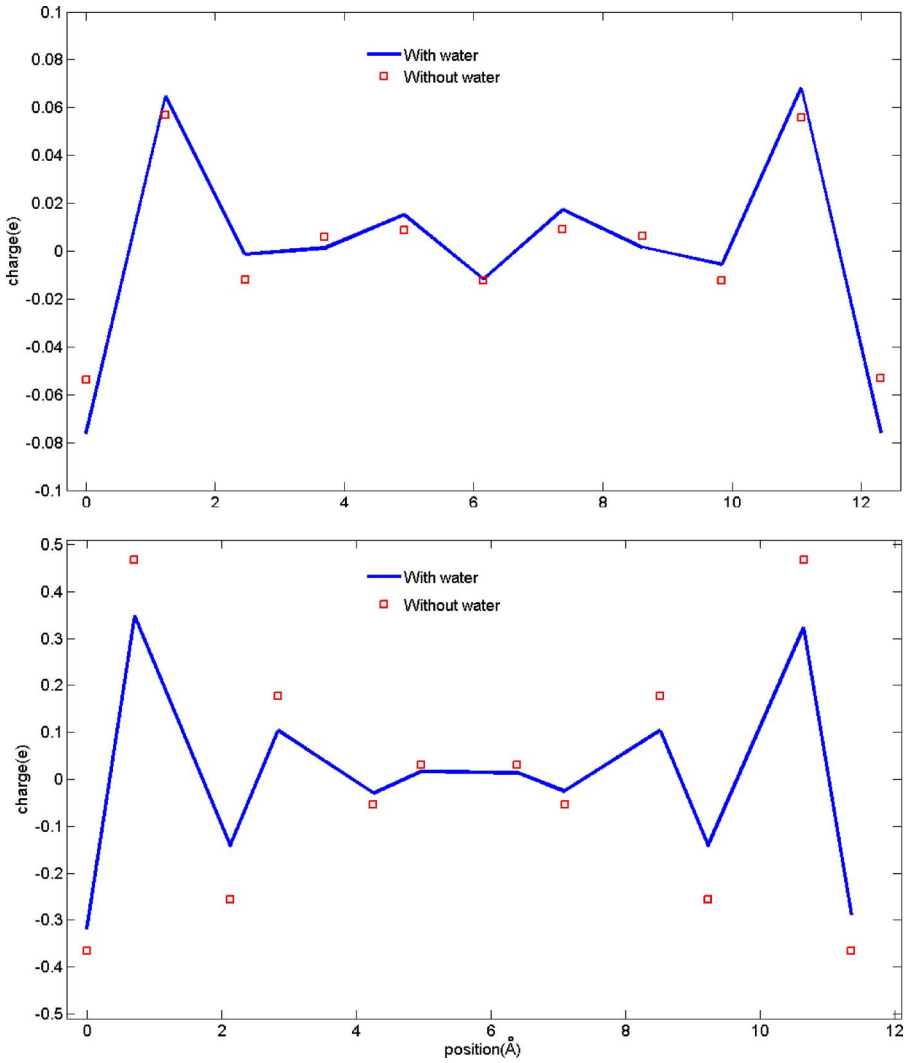

FIG. 2. Partial charge distribution on a (6,6) SWCNT (top) and a (10,0) SWCNT (bottom) along the tube axial direction. Solid line: water is included in the calculation and squares: no water is included in the calculation. A tube starts at 0 Å in the axial direction.

axial position. The squares in Fig. 2 denote partial charges computed without water molecules inside the tubes. For both the (6,6) and (10,0) tubes, we found that the magnitude of the charges at the tube ends is much greater compared to the charges in the middle region of the tube. The charges rapidly decrease in magnitude up to a distance of about 2 Å from the ends of the tube. Thus, the dominant contribution to the partial charge is from the end effects.

To calculate partial charges with water inside the tube, we obtained four different representative configurations that consisted of the SWCNT and water inside the tube from equilibrium MD simulations performed without partial charges on the carbon atoms. In two of the configurations, the water dipole vector points towards one end of the tube, and for the other two, the water dipole vector points towards the other end. DFT calculations were performed on the four representative configurations and the resulting average charges are shown as solid lines in Fig. 2. Snapshots from the MD simulations performed with the partial charges were again used in DFT calculations with new water orientations to test the effect of water orientation on the partial charges but the difference was found to be negligible. DFT calculations were also performed with water molecules in the first layer of the water near the tube entrance but the effect of the water in the first layer on the SWCNT partial charges was negligible. Due to the inhomogeneous distribution of water molecules (along the length of the tube) used in the calculations, the partial charge distribution on the nanotube deviates slightly from symmetry with respect to the center of the nanotube. The comparison of the solid line and the squares in Fig. 2 shows that water has a small effect on the electrostatic behavior of the (6,6) SWCNT and a considerable effect on the electrostatic behavior of the (10,0) SWCNT.

The effect of the tube chirality on the nanotube electrostatics can be understood by comparing the top and bottom figures in Fig. 2. The magnitude of the average partial charge (when water is included) at the ends of the zigzag SWCNT is approximately 4.5 times greater than that of the armchair SWCNT. This suggests that the electrostatic potential at the ends of the nanotube depends strongly on chirality. In a recent study,[20] it has been suggested that C–C triple bonds form at the end of a finite length armchair SWCNT but not in a zigzag open ended nanotube. When the C–C triple bonds are present, the electrons are shared and less localized, which causes the magnitude of the charges to be lower when compared to the case without the C–C triple bonds. When terminations are present at the ends of the tube, e.g., hydrogen passivation, the partial charges can be affected by the end

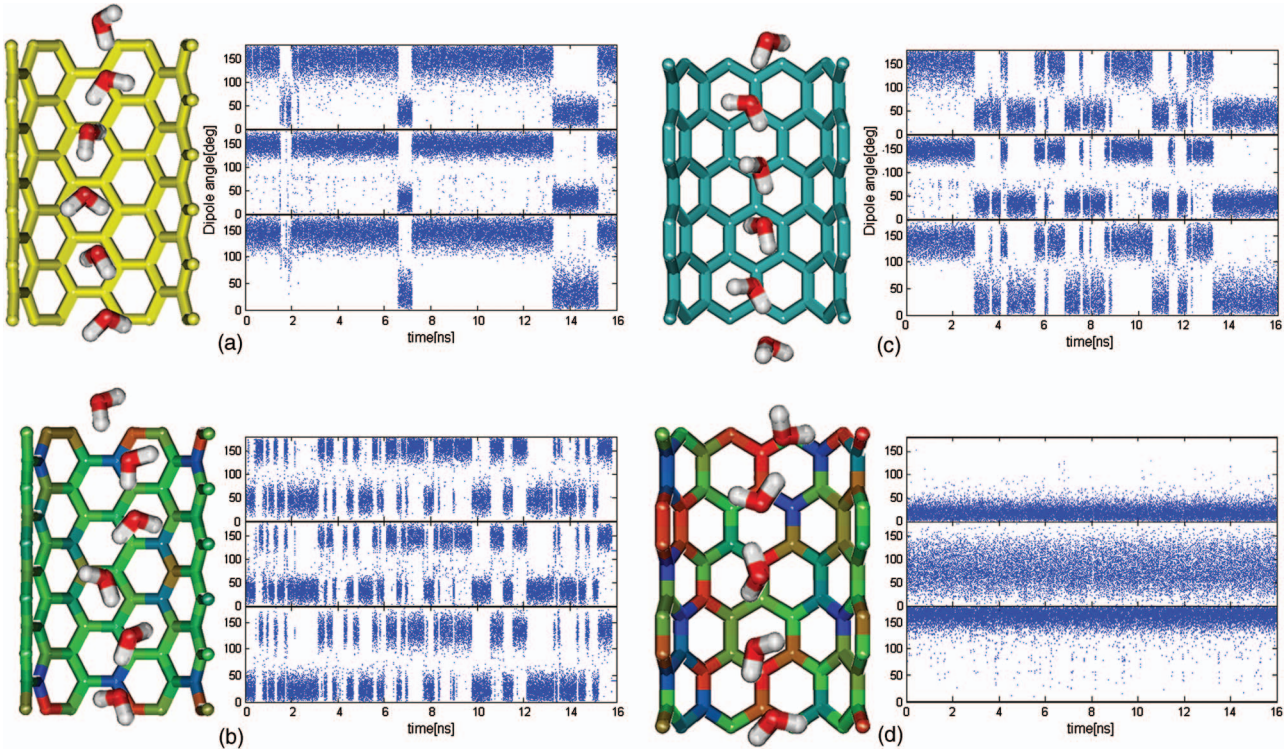

FIG. 3. (Color) A snap shot (left) and transient (right) of water dipole orientation in (a) an uncharged (6,6) SWCNT, (b) a partially charged (6,6) SWCNT, (c) an uncharged (10,0) SWCNT, and (d) a partially charged (10,0) SWCNT. Color of the SWCNTs in (b) and (d) represents the partial charge magnitude of each carbon atom. In the transient water dipole orientation figure (right), the top, middle, and bottom rows indicate the orientation of water molecues in top (1.8 nm from the top end), middle (0.5–0.68 nm), and bottom (1.8 nm from the bottom end) regions of tube, respectively. The water dipole orientation angle is defined as the angle between the water dipole vector and the tube axis z. 0° denotes the water dipole vector pointing towards the positive z axis. 90° denotes the water dipole vector pointing normal to the tube axis.

terminations and chirality could play a minor role. In this paper, in order to isolate the chirality effects alone, we used unterminated tubes.

B. Water dipole orientations

Using MD simulations, we investigated the dipole orientation of water confined to a nanotube for over 28 ns of simulation time. For both uncharged [see Fig. 3(a)] and partially charged [see Fig. 3(b)] (6,6) tubes, all the water molecules in the tube are oriented such that the dipole vectors of the water molecules point either towards the top water reservoir or towards the bottom water reservoir at any instant. Once a water molecule flips and reverses its orientation, all other water molecules flip simultaneously, due to the strong electrostatic coupling of the single-file water molecules, so that the orientation of all the water molecules remains the same. The flipping frequency of single-file water inside uncharged and partially charged (6,6) SWCNTs is considerably different. When the carbon atoms are assumed to not have any partial charges, all the dipole vectors in the tube point either towards the top or the bottom water reservior with the flipping occurring only six times during a 16 ns sampling time. In the presence of partial charges, the water dipole flips continuously as shown in Fig. 3(b).

We compared the water orientation obtained from the MD simulation with partial charges to that from *ab initio* MD simulation. Since the water orientation can be strongly affected by electrostatic interactions,[33,34] the comparison of water orientation from both the simulations would be a good way to evaluate our method of using one-way coupling between quantum and molecular dynamics because we have approximated the effect of the change in water configuration on the electronic structure of the SWCNTs by averaging over four representative configurations in obtaining the partial charges. Mann and Halls[17] observed water structure variation in a (6,6) SWCNT using *ab initio* MD simulation. Specifically, they examined the average water dipolar angle (see Fig. 4) which is defined as the average of angles between the water dipole vectors along the tube axial direction, $\theta_{\mu z}$. Mann and Halls pointed out that the average water dipole vector along a nanotube axis fluctuated with a range of roughly 20° from 135° during a 5 ps time period. Figure 4 shows a reasonable agreement for the average water dipole orientation as a function of time along the axis of the (6,6) tube suggesting that MD simulations with the partial charges could give similar results as *ab initio* MD simulation.

Unlike in the (6,6) tube, where the water structure is not significantly affected by the quantum charges except for the flipping frequency, the water structure in a partially charged (10,0) tube is markedly different. For the (10,0) SWCNT case, since the magnitude of the partial charges near the ends is high, a strong electrostatic field is generated at the ends of the tube. The direction and magnitude of the electrostatic field cause the water molecules at both the ends to be reoriented such that hydrogen atoms point towards the bath region [Fig. 3(d)]. Since the water dipoles at both ends point

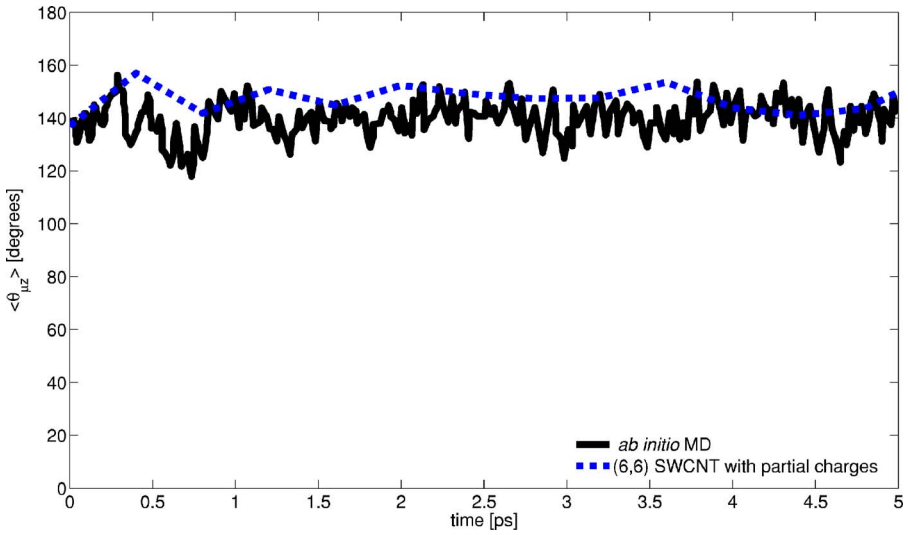

FIG. 4. Comparison of water orientation using our MD simulations with partial charges to that from *ab initio* MD (Ref. 17).

away from each other, the central water molecule forms an L defect.[35] For a single water chain, an L defect is formed when a water molecule acts as a hydrogen-bonding donor to its neighbors without accepting any hydrogen bonding.[36] Our calculations indicate that a water molecule in a single-file chain in the uncharged (10,0) tube donates and accepts about 0.86 hydrogen bonds, while the water molecule at the center of the partially charged (10,0) tube donates about 1.14 hydrogen bonds to its neighbors while accepting about 0.22 hydrogen bonds from the neighbors. This again suggests that an L defect is formed in the center of the (10,0) tube. It is also interesting to note that the orientation of water in a (10,0) nanotube containing an L defect is similar to the water orientation in an aquaporin-1 channel.[37]

C. Transport properties

The effect of the partial charges on water transport is evaluated in this section by computing the self-diffusion coefficient. Since water conducts through the SWCNTs by forming a single-file chain, we considered only water diffusion in the axial direction. The axial diffusion coefficient D_z of water is related to the slope of the water mean-squared displacement (MSD) by the well-known Einstein relation,

$$D_z = \frac{1}{2}\lim_{t\to\infty}\frac{\langle|r(t)-r(0)|^2\rangle}{\Delta t} = \frac{1}{2}\lim_{t\to\infty}\frac{\langle\Delta r^2\rangle}{\Delta t}, \qquad (1)$$

where $r(t)$ is the position vector at time t. Without partial charges, the value of the axial water self-diffusion coefficient in a (10,0) SWCNT is comparable to that of in a (6,6) SWCNT, which agrees well with a previous study[13] using a noncharged (6,6) SWCNT. Table I shows that the partial charges on the (6,6) SWCNT increase the diffusion coefficient by about 22%. For the (10,0) SWCNT case, water molecules in a partially charged nanotube have about 16% higher diffusion coefficient compared to water molecules in an uncharged nanotube.

We also examined the water molecule transport rate through the SWCNTs by measuring the translocation time, which is defined as the time taken for a water molecule to travel from one end of the tube to the other end of the tube. We observed that on an average 4.9 water molecules/ns passed through the uncharged (6,6) SWCNT with a translocation time average of 379.54 ps (Table I). The water transport rate is enhanced when partial charges are introduced into the system. For a (6,6) SWCNT, the number of translocation events per nanosecond increases by about 84.8% and the average time taken for crossing the nanotube decreases by about 130 ps when partial charges are considered. We observed similar trends in the transport rate of water molecules inside the (10,0) SWCNT, even though the water structure in the (10,0) tube is different. The number of translocations increases from 5.31 to. 6.69 ns^{-1} and the translocation time decreases from 353.96 to 263.99 ps. Though the magnitude of the charges in the (10,0) SWCNT is higher than that of the (6,6) SWCNT, the increase in the number of translocations due to the partial charges is less compared to that of the (6,6) tube.

The effect of the partial charges on the transport properties such as the diffusion coefficient and the translocation time can be understood in more detail by evaluating the energy barrier of the water molecules inside the tubes, which is discussed next.

D. Potential of mean force analysis

Using the potential of mean force (PMF) analysis, in this section, we try to understand the following observations, summarized in the previous sections: (i) water diffusion coefficient in the partially charged (6,6) tube is higher than that of the partially charged (10,0) tube even though the magni-

TABLE I. Single-file transport properties of water in uncharged and partially charged SWCNTs.

Chirality	Charge type	Diffusion coefficient (10^{-5} cm^2/s)	No. of translocation events (ns^{-1})	Translocation time (ps)
(6,6)	No partial charge	1.16±0.08	4.94	379.54
(6,6)	Partial charge	1.41±0.04	9.13	248.93
(10,0)	No partial charge	1.10±0.05	5.31	353.96
(10,0)	Partial charge	1.28±0.13	6.69	263.99

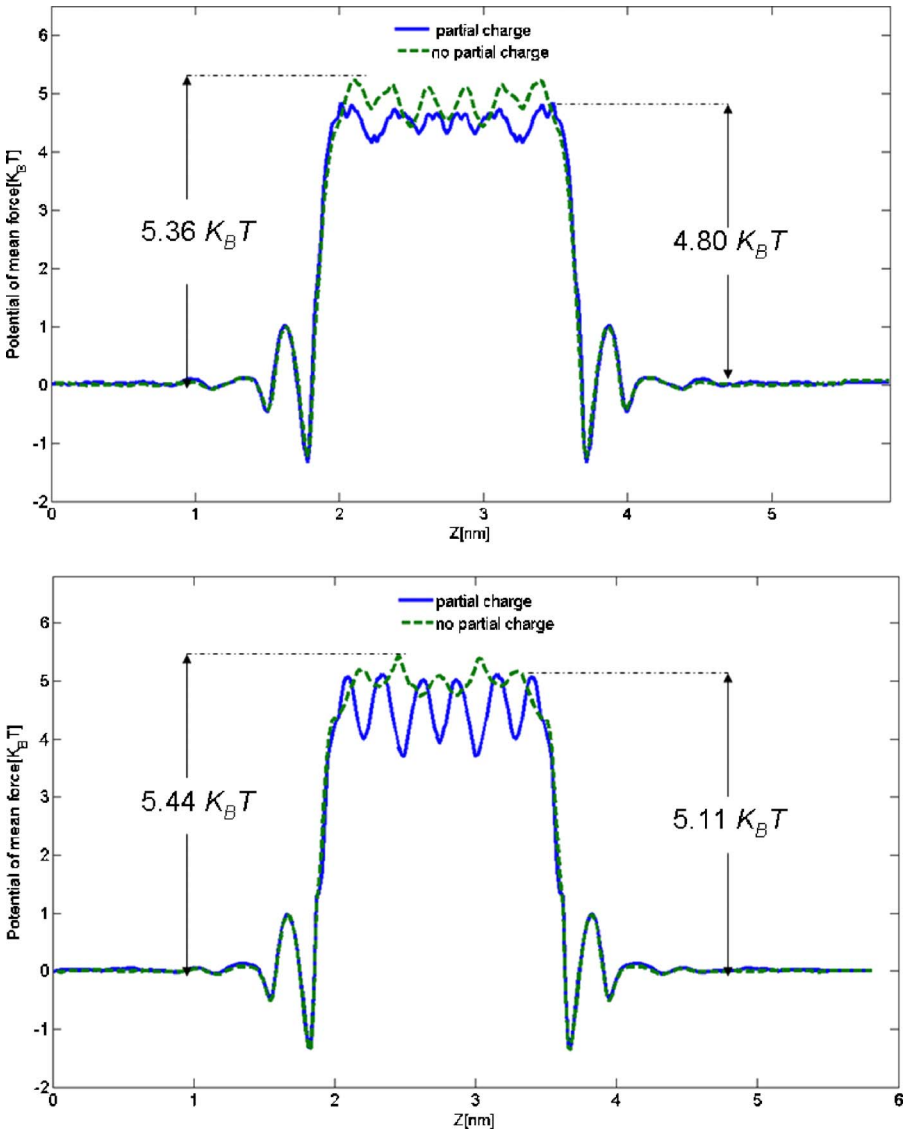

FIG. 5. PMF of water along the nanotube axial direction for a (6,6) SWCNT (top) and a (10,0) SWCNT (bottom). The (6,6) tube is located from 2.135 to 3.365 nm and the (10,0) tube is located from 2.182 to 3.318 nm.

tude of the partial charges is greater in the (10,0) tube, (ii) the water molecule in the center of the partially charged (10,0) tube forms an *L* defect, and (iii) the dipole orientation of the water molecules in the partially charged (6,6) tube flips continuously in the presence of partial charges.

When a water molecule *i* moves along the axial direction from z_0 to z, the work done, $W_i(z)-W_i(z_0)$, is computed by integrating the mean force $\langle F_i(z)\rangle$ acting on the water molecule along the nanotube axis contributed by all other atoms in the system averaged over all the configurations,[38] i.e.,

$$W_i(z) - W_i(z_0) = \int_{z_0}^{z} \langle F_i(z')\rangle dz', \tag{2}$$

where z_0 is the reference position (taken as the end of the simulation box) where the PMF is zero.[39] We obtained the mean force distribution by sampling the force experienced by the water molecules in a bin.[38]

As shown in Fig. 5, the energy barriers of the tubes are found to be $4.80k_BT$ and $5.11k_BT$ for the partially charged (6,6) and (10,0) SWCNTs, respectively. These water permeation barriers are of the same order of magnitude as that of in an aquaporin-1 water channel which is about $5k_BT$.[37,40] It should be noted that the water orientation and the permeation barrier in the (10,0) tube and the aquaporin-1 channel are similar, which makes the nanotube a promising candidate for biocompatible nanodevices.

To understand the energy barrier in more detail, we decomposed the PMF of water into contributions arising from different types of interactions such as the LJ and electrostatic interactions between water molecules and between water and nanotube. Figure 6 shows water-water and water-nanotube PMFs accounting for electrostatic and LJ effects. We can observe that the water-water electrostatic interaction and the water-nanotube LJ interaction form the energy barrier, while the water-water LJ interaction and the water-nanotube electrostatic interaction (present only in the case of partially charged tubes) make it favorable for the water molecule to reside inside the nanotube. Figures 6(a) and 6(e) show that the electrostatic interaction between the water molecules plays a crucial role in the development of the energy barrier. Partial charges on the wall attract water molecules towards the tube due to the electrostatic interaction between water and nanotube [see Figs. 6(c) and 6(g)] but they also increase the water-nanotube LJ barrier [see Figs. 6(d) and 6(h)].

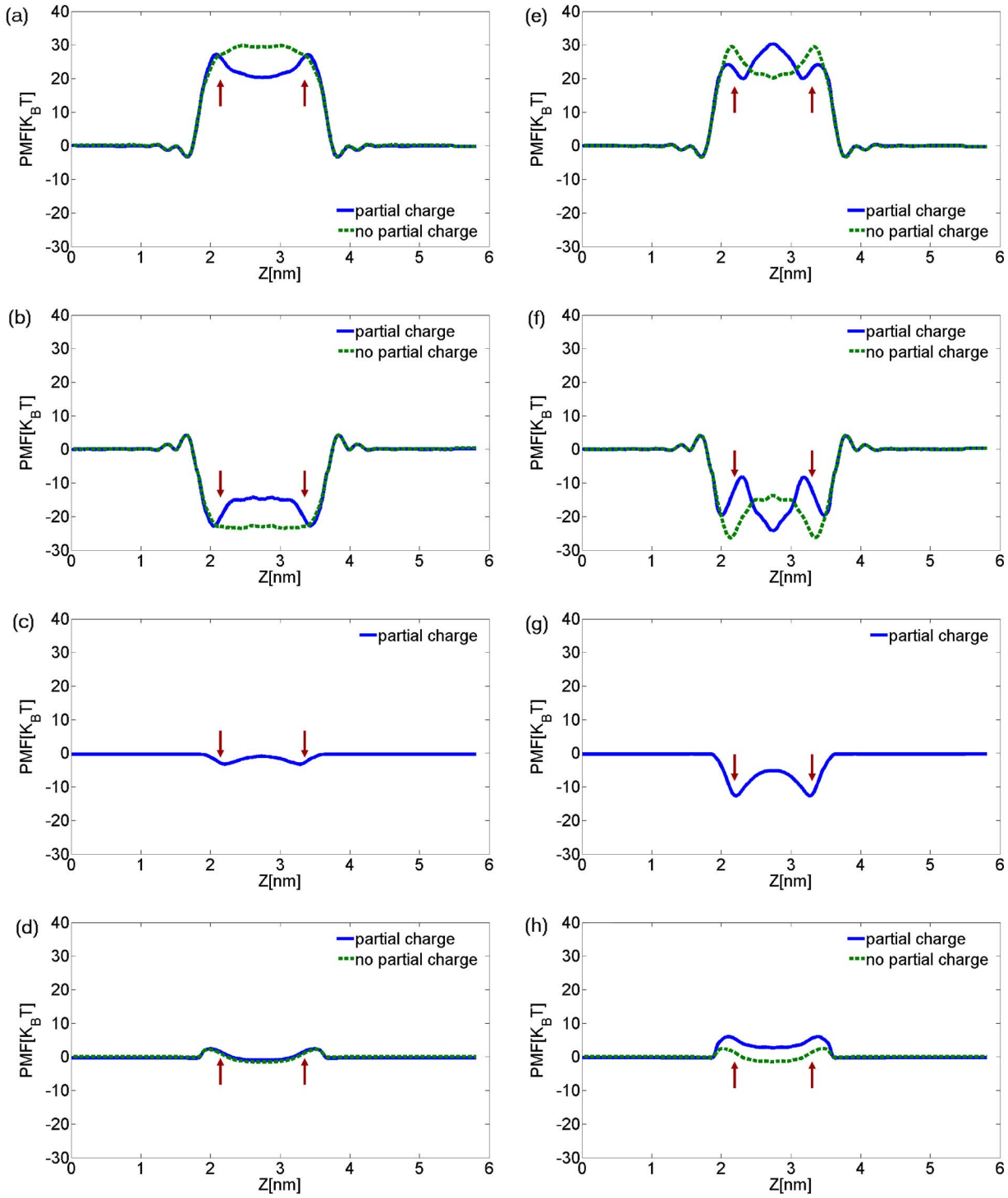

FIG. 6. Decomposition of the PMF of water into [(a) and (e)] water-water electrostatic interactions, [(b) and (f)] water-water LJ interactions, [(c) and (g)] water-nanotube electrostatic interactions, and [(d) and (h)] water-nanotube LJ interactions. The plots on the left [(a)–(d)] are for the (6,6) SWCNT and the plots on the right [(e)–(h)] are for the (10,0) SWCNT. The (6,6) tube is located from 2.135 to 3.365 nm and the (10,0) is located from 2.182 to 3.318 nm. The arrows denote the ends of the SWCNT.

The higher water diffusion coefficient in the partially charged (6,6) SWCNT compared to the partially charged (10,0) SWCNT can be understood by the comparison of the total PMF profiles of water for both tubes (Fig. 5). Water molecules inside the partially charged (10,0) tube experience a larger energy fluctuation compared to that inside the partially charged (6,6) tube. The energy barrier of the partially charged (10,0) tube is greater than that of the partially charged (6,6) tube. The larger energy barrier can lead to a less number of water molecules entering the partially charged (10,0) tube and the larger energy fluctuation inside the partially charged (10,0) tube leads to a lower diffusion coeffcient.

The water molecules in both the partially charged tubes have different orientations compared to that in the uncharged tubes as the water-nanotube electrostatic interaction is intro-

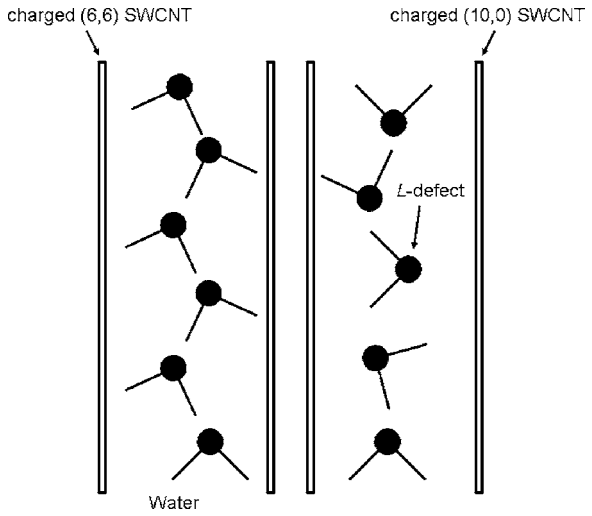

FIG. 7. Schematic of a single-file water chain in a partially charged (6,6) SWCNT (left) and in a partially charged (10,0) SWCNT (right). An L defect is observed in a single-file chain inside the charged (10,0) SWCNT.

duced to the system. In the partially charged (10,0) tube, since the magnitude of the partial charges is relatively large, the water-nanotube electrostatic interaction at the ends of the tube is considerable [Fig. 6(g)]. The substantial water-nanotube electrostatic interaction causes the water dipoles at the ends of the tube to be oriented such that the water hydrogens point towards the water reservoir. This water dipole reorientation results in an L defect at the tube center as shown in Fig. 7. Due to the reorientation of water dipoles in the mouth region, the water-water electrostatic barrier at the mouth reduces from about $29k_BT$ to $24k_BT$. The electrostatic barrier at the center of the tube increases back to about $30k_BT$ due to the formation of the L defect [Fig. 6(e)].

For the partially charged (6,6) SWCNT, since the magnitude of the partial charge is small, the water-nanotube electrostatic interaction is not strong enough to form an L defect. However, the water-nanotube electrostatic interaction, which is not present in the case of an uncharged tube, causes the water molecules to flip their orientation more frequently compared to the uncharged case. As a result, we see a more continuous flipping of water in the partially charged (6,6) tube. The water-water electrostatic interaction in the partially charged (6,6) tube is quite different from that of the partially charged (10,0) tube. The water-water electrostatic energy barrier starts to decrease at the mouth and it is lower in the center region of the tube compared to the uncharged (6,6) tube [Fig. 6(a)].

IV. CONCLUSIONS

Using (6,6) and (10,0) single-walled carbon nanotubes having a similar diameter and confinement effect but different electrostatic behaviors arising from their chiralities, we have shown that the chirality of a SWCNT has a significant influence on the single-file water structure and dynamics. The quantum partial charges, which capture the molecular electrostatic potential, induce relatively stronger wall-water electrostatic interactions at the ends of the tube and weaker electrostatic interactions at the center. Molecular dynamics simulations with these partial charges when compared with *ab initio* MD simulations give comparable water dipolar orientations inside the partially charged (6,6) tube. Water molecules in a partially charged nanotube have a higher transport rate, compared to water molecules in an uncharged tube. From PMF analysis, we found that a larger energy fluctuation inside the partially charged (10,0) tube induces a slower diffusion coeffcient when compared with the partially charged (6,6) tube. The substantial water-nanotube electrostatic interaction in the partially charged (10,0) tube changes the single-file water structure and gives rise to the formation of an L defect in the center of the nanotube.

ACKNOWLEDGMENTS

The authors would like to thank Dr. J. H. Park for many helpful discussions. This research was supported by NSF under Grant Nos. 0120978 (the Water CAMPWS Center at UIUC), 0325344, 0328162 (the nano-CEMMS Center at UIUC), and 0523435 and by NIH under Grant No. PHS 2 PN2 EY016570B.

[1] F. Balavoine, P. Schultz, C. Richard, V. Mallouth, T. W. Ebbesen, and C. Mioskowski, Angew. Chem., Int. Ed. **38**, 1912 (1999).
[2] S. Ghosh, A. K. Sood, and N. Kumar, Science **299**, 1042 (2003).
[3] P. A. Gordon and R. B. Saeger, Ind. Eng. Chem. Res. **38**, 4647 (1999).
[4] Q. Wang and J. K. Johnson, J. Phys. Chem. B **103**, 4809 (1999).
[5] M. Rzepka, P. Lamp, and M. A. de la Casa-Lillo, J. Phys. Chem. B **102**, 10894 (1998).
[6] C. V. Nguyen, L. Delzeit, A. M. Cassell, J. Li, J. Han, and M. Meyyappan, Nano Lett. **2**, 1079 (2002).
[7] M. S. P. Samson and P. C. Biggin, Nature (London) **414**, 156 (2001).
[8] K. Murata, K. Mitsuoka, T. Hirai, T. Walz, P. Agre, J. B. Hemann, A. Engel, and Y. Fujiyoshi, Nature (London) **407**, 599 (2000).
[9] G. Hummer, J. Rasaiah, and J. P. Noworya, Nature (London) **414**, 188 (2001).
[10] A. Kolesnikov, J.-M. Zanotti, C.-K. Loong, P. Thiyagarajan, A. Moravsky, R. O. Loutfy, and C. J. Burnham, Phys. Rev. Lett. **93**, 035503 (2004).
[11] M. J. O'Connell, P. Boul, L. Ericson, H. Chad, Y. Wang, E. Haroz, C. Kuper, J. Tour, K. Ausman, and R. E. Smalley, Chem. Phys. Lett. **342**, 265 (2001).
[12] M. P. Rossi, H. Ye, Y. Gogotsi, S. Babu, P. Ndungu, and J.-C. Bradley, Nano Lett. **4**, 989 (2004).
[13] R. J. Mashl, S. Joseph, N. R. Aluru, and E. Jakobsson, Nano Lett. **3**, 589 (2003).
[14] W. H. Noon, K. D. Ausman, R. E. Smalley, and J. Ma, Chem. Phys. Lett. **355**, 445 (2002).
[15] F. Moulin, M. Devel, and S. Picaud, Phys. Rev. B **71**, 165401 (2005).
[16] D. Lu, Y. Li, U. Ravaioli, and K. Schulten, J. Phys. Chem. B **109**, 11461 (2005).
[17] D. J. Mann and M. D. Halls, Phys. Rev. Lett. **90**, 195503 (2003).
[18] C. Dellago, M. M. Naor, and G. Hummer, Phys. Rev. Lett. **90**, 105902 (2003).
[19] S. Hou, Z. Shen, Z. Zhao, and Z. Xue, Chem. Phys. Lett. **373**, 308 (2003).
[20] C.-W. Chen and M.-H. Lee, Nanotechnology **15**, 480 (2004).
[21] M. J. Frisch, G. W. Trudes, H. B. Schlegel *et al.*, GAUSSIAN 03, Revision C.01, Gaussian, Inc., Wallingford, CT, 2004.
[22] J. Han and R. Jaffe, J. Chem. Phys. **108**, 2817 (1998).
[23] N. Sano, M. Chhowalla, D. Roy, and A. Amaratunga, Phys. Rev. B **66**, 133493 (2002).
[24] Y. Matsuo, K. Tahara, and E. Nakamura, Org. Lett. **5**, 3181 (2003).
[25] C. M. Breneman and K. B. Wiberg, J. Comput. Chem. **11**, 361 (1990).
[26] E. Lindahl, B. Hess, and D. van der Spoel, J. Mol. Model. **7**, 306 (2001).
[27] S. Joseph, R. J. Mashl, E. Jakobsson, and N. R. Aluru, Nano Lett. **3**, 1399 (2003).

[28] H. J. C. Berendsen, J. R. Grigera, and T. P. Straatsma, J. Phys. Chem. **91**, 6269 (1987).
[29] S. Mayamoto and P. A. Kollman, J. Comput. Chem. **13**, 952 (1993).
[30] S.-W. Chiu, S. Subramaniam, and E. Jakobsson, Biophys. J. **76**, 1939 (1999).
[31] H. J. C. Berendsen, J. P. M. Postma, A. DiNola, and J. R. Haak, J. Chem. Phys. **81**, 3684 (1984).
[32] G. Chen, Y. Guo, N. Karasawa, and W. A. Goddard III, Phys. Rev. B **48**, 13959 (1993).
[33] S. Vaitheeswaran, J. C. Rasiah, and G. Hummer, J. Chem. Phys. **121**, 7955 (2004).
[34] S. H. L. Klapp and M. Schoen, J. Chem. Phys. **117**, 8050 (2002).
[35] N. Bjerrum, Science **115**, 385 (1952).
[36] R. B. Best and G. Hummer, Proc. Natl. Acad. Sci. U.S.A. **102**, 6732 (2005).
[37] B. L. de Groot and H. Grubmüller, Curr. Opin. Struct. Biol. **15**, 176 (2005).
[38] R. Kjenllander and H. Greberg, J. Electroanal. Chem. **450**, 233 (1998).
[39] T. W. Allen, O. S. Anderson, and B. Roux, Proc. Natl. Acad. Sci. U.S.A. **101**, 117 (2004).
[40] M. J. Borgnia, and P. J. Agre, Proc. Natl. Acad. Sci. U.S.A. **98**, 2888 (2001).